Tailoring magnetic and electric resonances with dielectric nanocubes for broadband and high-efficiency unidirectional scattering

Yong Wang (王 勇), Xianghao Zeng (曾翔昊), Erchan Yang (杨二婵), Yonghua Lu (鲁拥华), Douguo Zhang (张斗国), and Pei Wang (王 沛)*

Department of Optics and Optical Engineering, Anhui Key Laboratory of Optoelectronic Science and Technology, University of Science and Technology of China, Hefei 230026, China

**Corresponding author: wangpei@ustc.edu.cn*

Received September 29, 2015; accepted November 19, 2015; posted online January 4, 2016

The interference of optically induced electric and magnetic resonances in high-refractive-index dielectric nanoparticles provides a new approach to control and shape the scattering patterns of light in the field of nanophotonics. In this Letter, we spectrally tune the electric and magnetic resonances by varying the geometry of a single isolated lead telluride (PbTe) dielectric nanocube. Then, we overlap the electric dipole resonance and magnetic dipole resonance to suppress backward scattering and enhance forward scattering in the resonance region. Furthermore, a broadband unidirectional scattering is achieved by structuring the dielectric nanocuboids as a trimer antenna.

OCIS codes: 160.3918, 290.0290, 050.6624.
doi: 10.3788/COL201614.011601.

Light scattering by metallic nanoparticles, thanks to localized surface plasmons resonance, has been widely studied[1] and shown many potential applications in the fields of nanophotonics, plasmonics, and metamaterials, such as nanoantennas[2], cloaking[3], sensing[4,5], photovoltaic devices[6], and metasurfaces[7,8]. Conventional approaches to the scattering control and shaping rely mostly on the electric responses of the nanostructures, while the magnetic responses are often ignored. As we know, introducing magnetic responses into the scattering system brings an extra dimension to engineer scattering patterns. However, natural materials that exhibit magnetic responses are very limited. To obtain artificial magnetic responses, various plasmonic structures, such as split-ring resonators[9], coupled nanorods[10–12], fishnets[13,14], and nanorings[15], are presented. However, all of these structures are always accompanied by metal intrinsic ohmic losses, which affect the performance of every plasmonic or metamaterial structure and hinder further possible applications[16].

Recently, it has been reported that high-refractive-index dielectric nanoparticles support electric and strong magnetic responses[17–22]. The magnetic dipole (MD) response in a dielectric nanoparticle originates from a circular current of the electric field inside the nanoparticles. The ability to possess electric and magnetic responses simultaneously in a nanoparticle is very interesting. According to Kerker's proposal[23] of backward scattering suppression and forward scattering enhancement, when electric dipole (ED) and MD are of the same magnitude and in phase, they will interfere destructively in the backward direction and constructively in the forward direction, thus leading to unidirectional scattering. A lot of work[24–33] has been done theoretically and experimentally to demonstrate this proposal. However, the frequency of unidirectional scattering is often not in the resonant region and consequently, the total scattering efficiency is inevitably relatively low. Thus, obtaining resonantly unidirectional scattering becomes more significant. By introducing a metallic core into a dielectric shell or splitting a nanocube with a gap, unidirectional scattering at the resonant frequency has been achieved[34–39]. However, introducing metallic components or a gap is not necessary for nanoparticles to achieve resonantly unidirectional scattering.

Here, a single isolated lead telluride (PbTe) dielectric nanocube is presented. The spectral positions of the ED resonance and MD resonance are tuned by tailoring the dielectric nanocube geometry. So, the ED resonance and MD resonance can be overlapped with the proper aspect ratio of a single isolated nanocuboid.

The scattering of the nanoparticles can be analytically calculated by the Mie theory[1,21]. The scattered field can be decomposed into a multiple series (the so-called Mie's expansion), characterized by the electric and magnetic Mie coefficients $\{a_n\}$ and $\{b_n\}$ (a_1 and b_1 being proportional to the ED and MD, a_2 and b_2 to the quadrupoles, and so on). For a nanoparticle smaller than the wavelength, the scattering field can be sufficiently described by the dipole components

$$I_s(\theta) \propto |3/2(a_1 + b_1 \cos\theta)|^2, \quad (1)$$

$$I_p(\theta) \propto |3/2(a_1 \cos\theta + b_1)|^2. \quad (2)$$

The forward scattering ($\theta = 0$) and backward scattering ($\theta = \pi$) intensities of interest can be obtained using

$$I_s(0) = I_p(0) = |3/2(a_1 + b_1)|^2, \quad (3)$$

$$I_s(\pi) = I_p(\pi) = |3/2(-a_1 + b_1)|^2. \quad (4)$$

From Eq. (4), it is clear that $I_s(\pi) = I_p(\pi) = 0$ when $a_1 = b_1$. This means that the backward scattering will be canceled out and light will be scattered only in the forward direction when the ED and MD components of the scattering field are in phase and of the same magnitude. In other words, high-efficiency unidirectional scattering is obtained.

Here, we consider a simple case of a single isolated PbTe dielectric cube with side length $d = 160$ nm and refractive index $n \approx 5.66$ illuminated by a plane wave in free space. As illustrated in Fig. 1(a), light is incident along the z-axis with the x-polarized electric field. The scattering spectra and electromagnetic field distribution can be calculated through finite-difference time-domain method (Lumerical, Solutions). Figure 1(a) shows the scattering spectra with MD resonance at 1105 nm, ED resonance at 821 nm and magnetic quadrupole (MQ) resonance at 730.8 nm, corresponding to the electromagnetic field distribution in Figs. 1(b), 1(c), and 1(d).

As we know, the resonance wavelength of a nanoparticle is related to its size[18,29]. For a nanocuboid, its size is governed by three individual geometric parameters: l, w, and h, corresponding to the length along the x-axis, the width along the y-axis, and the height along the z-axis. Now, we shrink one side of the single isolated nanocuboid but leave the other two sides unchanged to tailor the ED resonance and MD resonance. Figure 2 shows that the

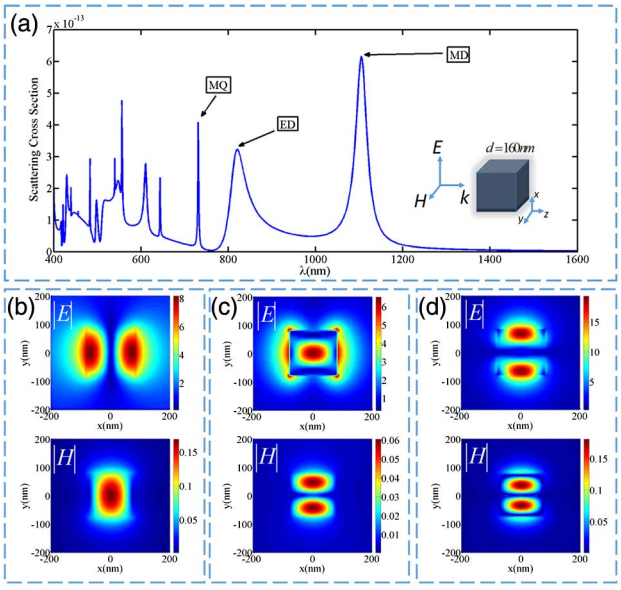

Fig. 1. (a) Numerical simulation result of the scattering spectra. The inset shows a schematic diagram of the problem. (b) Electromagnetic field distribution at MD resonance ($\lambda = 1105$ nm). (c) Electromagnetic field distribution at ED resonance ($\lambda = 821$ nm). (d) Electromagnetic field distribution at MQ resonance ($\lambda = 730.8$ nm).

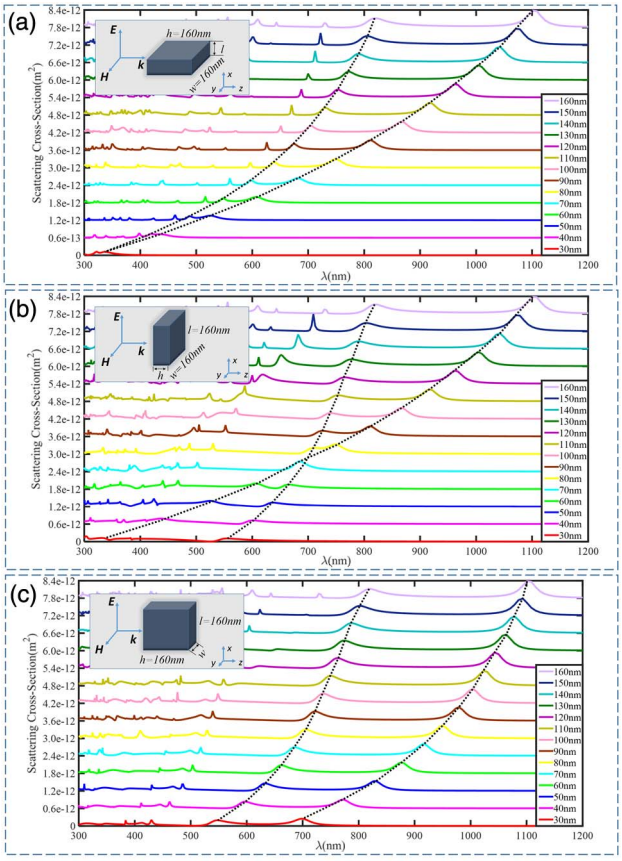

Fig. 2. Scattering spectra of the nanocuboid with different h, l, and w ranging from 160 to 30 nm. The inset shows the schematic diagram of the problem.

spectra positions of the MD resonance, ED resonance, and MQ resonance all blueshift as one side decreases. Meanwhile, the MD resonance shifts faster than the ED resonance, and the two resonances get closer. However, there are some differences when we change different sides. It can be seen from Fig. 2(a) that when we vary h from 160 to 30 nm with $w = l = 160$ nm, the MD resonance and ED resonance overlap with each other at h between 70 and 80 nm at the optical frequency. It is similar when we change l. Although the two dipole resonances cannot overlap at the optical frequency, they could overlap at the ultraviolet frequency, which can be seen in Fig. 2(b). However, it can be seen from Fig. 2(c) that the two dipole resonances can hardly overlap when w changes. So, here are two ways for a nanocuboid to obtain resonantly unidirectional scattering: (1) shrink the side that is parallel to the wave vector $\boldsymbol{k}$[40], and (2) shrink the side that is parallel to the electric field $\boldsymbol{E}$.

After further simulations, we find that when (1) $l = 160$ nm, $w = 160$ nm, and $h = 72$ nm or (2) $l = 32$ nm, $w = 160$ nm, $h = 160$ nm, the MD and ED overlap quite well with each other. The aspect ratios are about 1:1:0.45 and 0.2:1:1, respectively. From Figs. 3(a) and 4(a), it is clear that the nanocuboid is resonant at 693 and 354 nm, respectively. The scattering far fields shown in Figs. 3(b) and 4(b) agree well with Kerker's proposal.

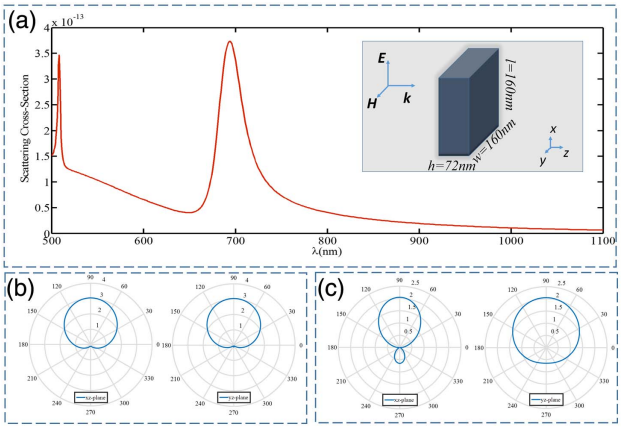

Fig. 3. (a) Scattering spectra of the nanocuboid with $l = w =$ 160 nm and $h = 72$ nm. The inset shows the schematic diagram of the geometry. The far-field scattering pattern at (b) the resonance frequency ($\lambda = 693$ nm) and (c) the off-resonance frequency ($\lambda = 800$ nm).

Now, high-efficiency unidirectional scattering is fulfilled by a single isolated nanocuboid at the resonance frequency. According to characterizing directivity (D) of the antenna[2],

$$D = \frac{4\pi \,\mathrm{Max}[p(\theta,\varphi)]}{P_{\mathrm{rad}}}, \qquad P_{\mathrm{rad}} = \int_{\Omega} p\{\theta,\varphi)\mathrm{d}\Omega, \tag{5}$$

where P_{rad} is the integrated radiated power, θ and φ are spherical angles, and $p(\theta,\varphi)$ is the radiated power in the given direction θ and/or φ. Here, for the nanocuboid, the directivity (D) is about 3.0463 from Fig. 3(b) and 3.1114 from Fig. 4(b) at the resonance frequency compared to 2.049 and 2.117 at the off-resonance frequency shown in Figs. 3(c) and 4(c). The backward scattering of case (2), shown in Figs. 4(b) and 4(c), is not completely diminished compared to case (1), which is shown in Fig. 3(b).

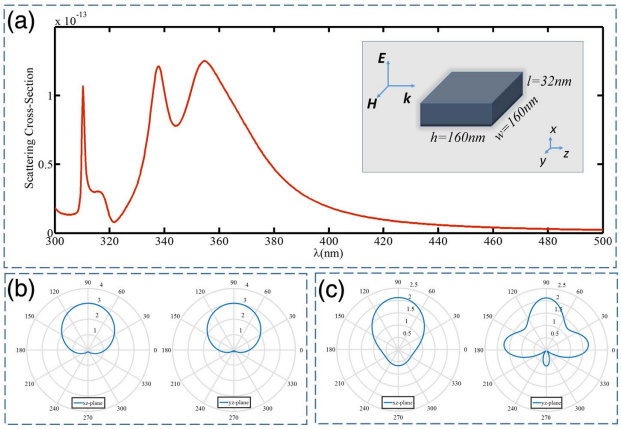

Fig. 4. (a) Scattering spectra of the nanocuboid with $h = w =$ 160 nm and $l = 32$ nm. The inset shows the schematic diagram of the geometry. The far-field scattering pattern at (b) the resonance frequency ($\lambda = 354$ nm) and (c) the off-resonance frequency ($\lambda = 343$ nm).

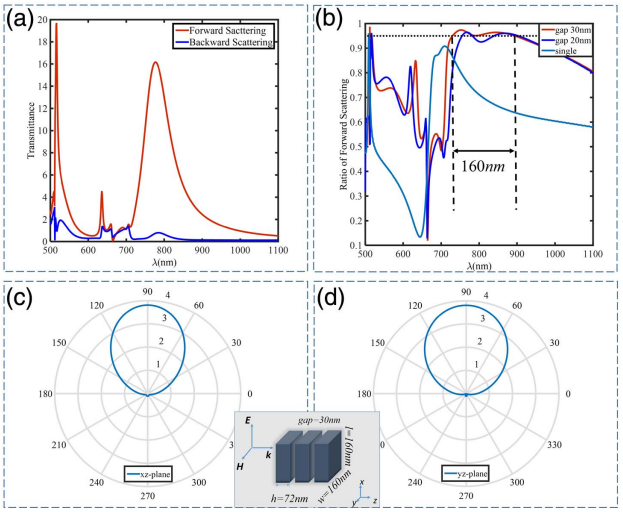

Fig. 5. (a) Transmittance of forward scattering (red line) and backward scattering (blue line) of 30 nm gap. (b) Ratio of forward scattering to total scattering. Red solid line corresponds to the case of the 30 nm gap, the dark blue corresponds to the 20 nm gap, the light blue to the single isolated nanocuboid, and the dashed line to the ratio of 95%. Far-field scattering pattern at 777.4 nm in (c) xz-plane and (d) yz-plane. The inset shows the schematic of the problem.

The reason might be that the MQ resonance at 338 nm is so close to the dipole resonance at 354 nm that it will contribute to the far-field scattering, thus leading to an unpleasant scattering pattern. From Fig. 4(c), it can be clearly seen that the MQ resonance greatly modifies the scattering patterns at 343 nm.

The directivity of a single isolated nanocuboid, however, is not high as we want, and the frequency of the unidirectional scattering is confined at a very narrow resonant region, which may hinder further possible applications. Inspired by the work in Refs. [35,41], the directivity of an antenna can be improved by arranging the nanoparticles in a chain. Now, we arrange the nanocuboid with $l = 160$ nm, $w = 160$ nm, and $h = 72$ nm into a linear trimer with a 30 nm gap. The trimer is illuminated by a plane wave with an x-polarized electric field from the $+z$-direction in free space. From the transmittance spectra shown in Fig. 5(a), the trimer is highly transmissive over a wide frequency band in the resonance region. After further calculation, in Fig. 5(b), over 95% of energy is scattered forward, from 730 to 890 nm, which means that 160 nm bandwidth high-efficiency unidirectional scattering is obtained. Figures 5(c) and 5(d) shows the far-field scattering pattern; the directivity ($D \approx 3.8078$) is enhanced compared to an isolated nanocuboid.

In conclusion, we demonstrate that the ED resonance and MD resonance of a single isolated nanocuboid can be spectrally tuned to overlap with each other by varying the aspect ratio of the nanocuboid. The ability to tailor the ED resonance and MD resonance provides an opportunity to control the far-field scattering pattern. High-efficiency unidirectional scattering at the resonance

frequency can be obtained by the nanocuboid through two ways: (1) shrink the side parallel to $\boldsymbol{k}$ with aspect ratio 1:1:0.45, and (2) shrink the side parallel to $\boldsymbol{E}$ with aspect ratio 0.2:1:1. By arranging the nanocuboid into a linear trimer, a bandwidth of 160 nm unidirectional scattering with a higher directivity of 3.8 is achieved. This work may offer a way for designing very efficient and low-loss optical nanoantennas, but first, further experimental work will need to be done.

This work was supported by the National Key Basic Research Program of China (No. 2012CB921900) and the National Natural Science Foundation of China (Nos. 61377053, 11274293, and 11374286).

References

1. C. F. Bohren and D. R. Huffman, *Absorption and Scattering of Light by Small Particles* (Wiley, New York, 1983).
2. L. Novotny and N. van Hulst, Nat. Photon. **5**, 83 (2011).
3. A. Alù and N. Engheta, Phys. Rev. Lett. **102**, 1 (2009).
4. A. V. Kabashin, P. Evans, S. Pastkovsky, W. Hendren, G. A. Wurtz, R. Atkinson, R. Pollard, V. A. Podolskiy, and A. V. Zayats, Nat. Mater. **8**, 867 (2009).
5. W. Wei, J. Nong, L. Tang, G. Zhang, X. Jiang, and Y. Zhu, Chin. Opt. Lett. **13**, 082801 (2015).
6. H. A. Atwater and A. Polman, Nat. Mater. **9**, 205 (2010).
7. N. Meinzer, W. L. Barnes, and I. R. Hooper, Nat. Publ. Gr. **8**, 889 (2014).
8. O. You, B. Bai, and X. Li, Chin. Opt. Lett. **12**, 082401 (2014).
9. J. B. Pendry, A. J. Holden, D. J. Robbins, and W. J. Stewart, IEEE Trans. Microw. Theory Tech. **47**, 2075 (1999).
10. G. Dolling, C. Enkrich, M. Wegener, J. F. Zhou, C. M. Soukoulis, and S. Linden, Opt. Lett. **30**, 3198 (2005).
11. V. M. Shalaev, W. Cai, U. K. Chettiar, H.-K. Yuan, A. K. Sarychev, V. P. Drachev, and A. V. Kildishev, Opt. Lett. **30**, 3356 (2005).
12. M. Zhong, Chin. Opt. Lett. **12**, 041601 (2014).
13. S. Zhang, W. Fan, N. C. Panoiu, K. J. Malloy, R. M. Osgood, and S. R. J. Brueck, Phys. Rev. Lett. **611**, 1 (2005).
14. J. Valentine, S. Zhang, T. Zentgraf, E. Ulin-Avila, D. A. Genov, G. Bartal, and X. Zhang, Nature **455**, 376 (2008).
15. F. Shafiei, F. Monticone, K. Q. Le, X.-X. Liu, T. Hartsfield, A. Alù, and X. Li, Nat. Nanotechnol. **8**, 959 (2013).
16. J. B. Khurgin, Nat. Nanotechnol. **10**, 2 (2015).
17. A. B. Evlyukhin, S. M. Novikov, U. Zywietz, R. L. Eriksen, C. Reinhardt, S. I. Bozhevolnyi, and B. N. Chichkov, Nano Lett. **12**, 3749 (2012).
18. A. Garcia-Etxarri, R. Gomez-Medina, L. S. Froufe-Perez, C. Lopez, L. Chantada, and F. Scheffold, Opt. Express **19**, 4815 (2011).
19. A. I. Kuznetsov, A. E. Miroshnichenko, Y. H. Fu, J. Zhang, and B. Luk'yanchuk, Sci. Rep. **2**, 492 (2012).
20. M. K. Schmidt, R. Esteban, J. J. Saenz, I. Suárez-Lacalle, S. Mackowski, and J. Aizpurua, Opt. Express **20**, 930 (2012).
21. U. Zywietz, M. K. Schmidt, A. B. Evlyukhin, C. Reinhardt, J. Aizpurua, and B. N. Chichkov, ACS Photon. **2**, 913 (2015).
22. J. H. Yan, P. Liu, Z. Y. Lin, H. Wang, H. J. Chen, C. X. Wang, and G. W. Yang, Nat. Commun. **6**, 7042 (2015).
23. M. Kerker, D. Wang, and C. L. Giles, J. Opt. Soc. Am. **73**, 765 (1983).
24. Y. H. Fu, A. I. Kuznetsov, A. E. Miroshnichenko, Y. F. Yu, and B. Luk'yanchuk, Nat. Commun. **4**, 1527 (2013).
25. J. M. Geffrin, B. García-Cámara, R. Gómez-Medina, P. Albella, L. S. Froufe-Pérez, C. Eyraud, A. Litman, R. Vaillon, F. González, M. Nieto-Vesperinas, J. J. Sáenz, and F. Moreno, Nat. Commun. **3**, 1171 (2012).
26. S. Person, M. Jain, Z. Lapin, J. Jose, G. Wicks, and L. Novotny, Nano Lett. **13**, 1806 (2013).
27. I. Liberal, I. Ederra, R. Gonzalo, and R. W. Ziolkowski, J. Opt. **17**, 72001 (2015).
28. J. A. Schuller, R. Zia, T. Taubner, and M. L. Brongersma, Phys. Rev. Lett. **99**, 1 (2007).
29. B. S. Luk'yanchuk, N. V. Voshchinnikov, R. Paniagua-Domínguez, and A. I. Kuznetsov, ACS Photon. **2**, 993 (2015).
30. W. Liu, Opt. Express **23**, 14734 (2015).
31. D. Sikdar, W. Cheng, and M. Premaratne, J. Appl. Phys. **117**, 083101 (2015).
32. S. Zhang, R. Jiang, Y.-M. Xie, Q. Ruan, B. Yang, J. Wang, and H.-Q. Lin, Adv. Mater. **27**, 02917 (2015).
33. H. Wang, P. Liu, Y. Ke, Y. Su, L. Zhang, N. Xu, S. Deng, and H. Chen, ACS Nano. **9**, 436 (2015).
34. S. Campione, L. I. Basilio, L. K. Warne, and M. B. Sinclair, Opt. Express **23**, 2293 (2015).
35. W. Liu, A. E. Miroshnichenko, D. N. Neshev, and Y. S. Kivshar, ACS Nano. **6**, 5489 (2012).
36. W. Liu, A. E. Miroshnichenko, D. N. Neshev, and Y. S. Kivshar, Phys. Rev. B **86**, 081407 (2012).
37. W. Liu, A. E. Miroshnichenko, R. F. Oulton, D. N. Neshev, O. Hess, and Y. S. Kivshar, Opt. Lett. **38**, 2621 (2013).
38. W. Liu, J. Zhang, B. Lei, H. Ma, W. Xie, and H. Hu, Opt. Express **22**, 16178 (2014).
39. W. Liu, A. E. Miroshnichenko, and Y. S. Kivshar, Chin. Phys. B **23**, 047806 (2014).
40. I. Staude, A. E. Miroshnichenko, M. Decker, N. T. Fofang, S. Liu, E. Gonzales, J. Dominguez, T. S. Luk, D. N. Neshev, I. Brener, and Y. Kivshar, ACS Nano **7**, 7824 (2013).
41. Z. Xi, Y. Lu, W. Yu, P. Yao, P. Wang, and H. Ming, Opt. Express **21**, 29365 (2013).